HHS Public Access

Author manuscript

Curr Biol. Author manuscript; available in PMC 2022 January 11.

Published in final edited form as:

Curr Biol. 2021 January 11; 31(1): 128–137.e5. doi:10.1016/j.cub.2020.10.001.

Coordinate Regulation of Ribosome and tRNA Biogenesis Controls Hypoxic Injury and Translation

Omar A Itani[1,2], **Xuefei Zhong**[3], **Xiaoting Tang**[3], **Barbara A. Scott**[1,2], **Jun Yi Yan**[1,2,4], **Stephane Flibotte**[5], **Yiting Lim**[6], **Andrew C. Hsieh**[3,6,7], **James E. Bruce**[3], **Marc Van Gilst**[1,2], **C. Michael Crowder**[1,2,3,*]

[1]Department of Anesthesiology and Pain Medicine, University of Washington, 1959 NE Pacific Street, Seattle, WA 98195-6540, USA

[2]Mitochondria and Metabolism Center, University of Washington, 850 Republican Street, Seattle, WA 98105, USA

[3]Department of Genome Sciences, University of Washington, 3720 15th Ave NE, Seattle, WA 98105, USA

[4]Department of Anesthesiology, Central Hospital of Changdian, Dandong, Liaoning Province, 118214, China

[5]Life Sciences Institute, University of British Columbia, 2350 Health Sciences Mall Vancouver, BC V6T 1Z3, Canada

[6]Division of Human Biology, Fred Hutchinson Cancer Research Center, 1100 Fairview Ave. N, Seattle, WA 98109, USA

[7]Department of Medicine, University of Washington, 1959 NE Pacific Street, Seattle, WA 98195-6420, USA

Summary

The translation machinery is composed of a myriad of proteins and RNAs whose levels must be coordinated to produce efficiently proteins without wasting energy or substrate. However, protein synthesis is clearly not always perfectly tuned to its environment as disruption of translation machinery components can lengthen lifespan and stress survival. While much has been learned from bacteria and yeast about translational regulation, much less is known in metazoans. In a

*Corresponding author and Lead Contact: cmc53@uw.edu.

Author Contributions: OAI – performed all of the genetic experiments, helped design all experiments, wrote the paper; XZ – performed the proteomic experiments and analysis; XT – performed the proteomic experiments and analysis; BAS – performed many of the hypoxic sensitivity experiments, performed the in vivo SILAC labelling and protein extractions for the proteomic work, and performed portions of the ^{35}S-methionine labelling experiments; JYY – performed several of the hypoxic sensitivity experiments; SF – analyzed the whole genome sequences to identify candidate mutations; YL – performed, analyzed, and interpreted the polysome profiling experiments; ACH – helped design and interpret the polysome profiling experiments; JEB – helped design and interpret the proteomic experiments; MVG – helped design all of the experiments and helped write the paper; CMC – helped design all experiments and wrote the paper.

Declaration of Interests: The authors declare no competing interests.

screen for mutations protecting *C. elegans* from hypoxic stress, we isolated multiple genes impacting protein synthesis: a ribosomal RNA helicase gene, tRNA biosynthesis genes, and a gene controlling amino acid availability. To define better the mechanisms by which these genes impact protein synthesis, we performed a second screen for suppressors of the conditional developmental arrest phenotype of the RNA helicase mutant and identified genes involved in ribosome biogenesis. Surprisingly, these suppressor mutations restored normal hypoxic sensitivity and protein synthesis to the tRNA biogenesis mutants, but not to the mutant reducing amino acid uptake. Proteomic analysis demonstrated that reduced tRNA biosynthetic activity produces a selective homeostatic reduction in ribosomal subunits, thereby offering a mechanism for the suppression results. Our study uncovers an unrecognized higher order translation regulatory mechanism in a metazoan whereby ribosome biogenesis genes communicate with genes controlling tRNA abundance matching the global rate of protein synthesis with available resources.

Graphical Abstract

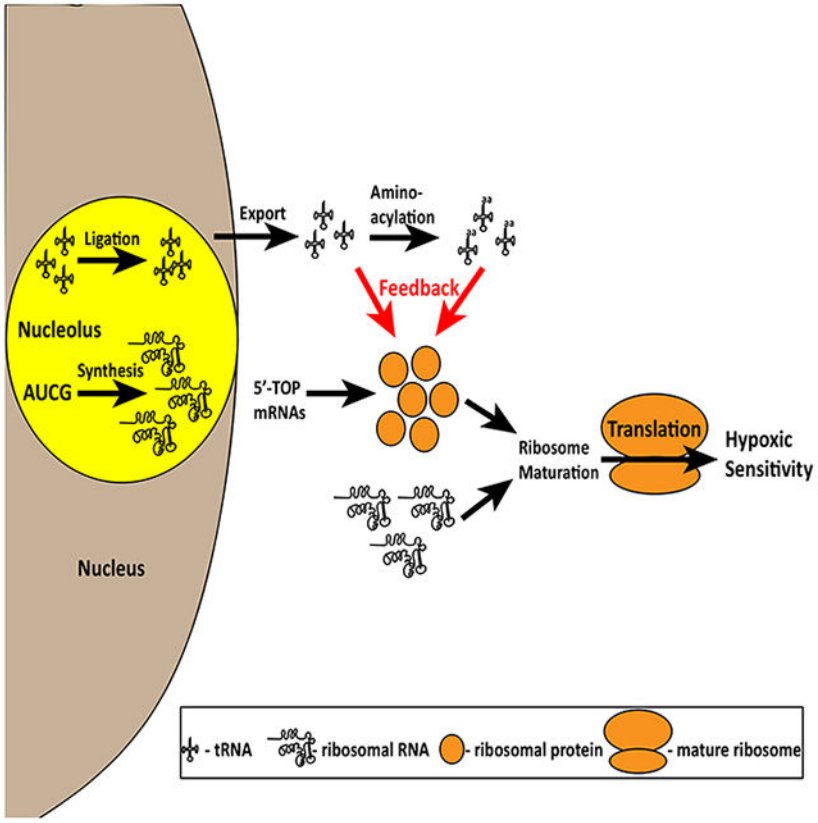

eTOC Blurb

In a screen in the nematode *C. elegans* for mutants that are resistant to hypoxic cellular injury, Itani *et al.* isolate mutations in multiple genes in the translation machinery. Subsequent genetic and proteomic experiments lead to our serendipitous discovery of a feedback mechanism between tRNA and ribosome biogenesis.

Introduction

Global protein synthesis rates are tightly regulated to match the anabolic needs of a cell to its available substrates and energetics. When oxygen is limiting, ATP levels fall and global translation rates are downregulated by a set of complex mechanisms that are still being elucidated [1–5]. This downregulation of translation is presumed to be adaptive and cytoprotective by allowing the unused ATP to be diverted for maintenance of basal metabolic needs until oxygen is restored. We have previously performed unbiased genetic screens in *C. elegans* and found that mutants and RNAis that reduce protein synthesis protect animals from hypoxic injury [6, 7]. However, a systematic examination of the role of translation and translation factors in hypoxic sensitivity found no relationship between oxygen consumption and hypoxic sensitivity [8]. Thus, while reducing the normal function of multiple components of the translation machinery is clearly hypoxia protective, the precise mechanism is far from understood. Contributing to this incomplete understanding is the fact that most of what we know about translation has been gained by studies in bacteria and yeast. It is likely that translational regulatory mechanisms have become more complex in multicellular organisms; thus, studies of translational regulatory mechanisms in higher eukaryotes is needed in general and in particular to understand better how the translation machinery regulates hypoxic injury.

We report here that in an unbiased genetic screen for genes involved in hypoxic injury, we identified numerous genes involved in protein synthesis. The extraordinary bias for translation mutants further reinforces the profoundly impactful role that the translation machinery has on hypoxic sensitivity. The isolation of translation mutants with easy to assay temperature sensitive growth phenotypes presented an excellent opportunity to use *C. elegans* genetics to further elucidate pathways involved in the regulation of eukaryote protein synthesis and their role in hypoxic injury. To this end, we carried out a second screen to isolate suppressors of one of the protein synthesis mutants. Our suppressors reveal new eukaryote-specific regulatory pathways controlling ribosome biogenesis and provide intriguing new insight into the regulation of protein synthesis in animals.

Results

DDX-52 is required for hypoxia sensitivity and for development at high temperature

Towards the goal of identifying genes that impact survival after hypoxic injury, we performed a forward genetic screen in the nematode *C. elegans* for mutations conferring hypoxia resistance. We mutated wild type *C. elegans* and screened through the F2 progeny for mutant animals that were able to recover from a hypoxic incubation that is lethal for wild type animals. A combination of genetic mapping, whole genome sequencing, candidate testing, complementation, and transformation rescue demonstrated that the hypoxia resistant *gc51* mutation isolated in our screen is a loss of function allele of *ddx-52* (Figure 1A–1C). *ddx-52* encodes a conserved DEAD/DEAH-box-containing ATP-dependent RNA helicase (Figure 1D). *gc51* is a missense mutation (G173R) in the ATP binding motif of DDX-52 (Figure 1D). The yeast ortholog of DDX-52 is ROK1, which has been shown to be essential for ribosome biogenesis; mutations in the ATP binding motif of ROK1 block 60S ribosomal subunit assembly [9]. As has been shown for ROK1 [10], DDX-52::GFP is ubiquitously

expressed and localizes to the nucleolus (Figure 1E and 1F), consistent with a similar role of DDX-52 in ribosome biogenesis. Besides hypoxia resistance, loss of DDX-52 activity caused a second phenotype, early developmental arrest and death when grown at high temperature (Figure 1G–1I, Table S1). *ddx-52(gk409936)*, a previously isolated *ddx-52* allele, has a stop codon (Y353Ochre) that would result in a truncated protein lacking the C-terminal helicase domain and is a presumptive null allele [11]. *ddx-52*(*gk409936*) shares the temperature-dependent developmental arrest and hypoxia resistance phenotypes and fails to complement *gc51* for both phenotypes (Table S1). Overexpression of wild type DDX-52 suppressed both the hypoxia resistance and temperature-induced developmental arrest phenotypes (Figure 1C, Table S1) of *ddx-52(gc51)*. Based on the phenocopy of *gc51* and *gk409936*, the failure to complement, the phenotypic rescue of *gc51* phenotypes by expression of wild type DDX-52, and the nature of the mutations in *gc51* and *gk409936*, we conclude that both the hypoxia resistance and temperature-dependent developmental arrest phenotypes of these mutants are due to loss of DDX-52 function.

Suppressors of *ddx-52(lf)* developmental arrest

To understand better the regulation and function of DDX-52, we performed a genetic suppressor screen to identify mutations that can ameliorate the temperature-induced developmental arrest phenotype of DDX-52 loss-of-function (Figure 2A). Accordingly, we mutated *ddx-52(gc51)* animals and screened F2 progeny for mutations that allowed for development to late larval and adulthood at higher temperature (26°C). Through genetic mapping, sequencing, and candidate testing, we identified seven suppressor mutations in five different genes (Figure 2B and Table S2). With the exception of *ulp-4*, which encodes a SUMO specific peptidase, the remaining four *ddx-52*(lf) suppressor genes have known functions in ribosome biogenesis, thus confirming the primary function of DDX-52 in this cellular function. A description of the suppressor genes and how the assignment was made of the suppressor mutations to those genes follows.

Two independent suppressor mutations, *gc56* and *gc57*, were identified in *larp-1*. LARP-1 is orthologous to mammalian LARP1, which binds to and inhibits the translation of terminal oligopyrimidine motif (TOP) mRNAs including those that encode ribosomal proteins [12–14]. An independent *larp-1* loss of function allele *(q783)* and *larp-1(RNAi)* each similarly suppressed the temperature-induced arrest of *ddx-52(lf)* (Figure S1A and S1B). Thus, *larp-1(gc56)* and *larp-1(gc57)* behave as loss of function alleles. *gc53* was identified as a 155 bp deletion in *ncl-1. ncl-1* encodes an established repressor of ribosome biogenesis and maturation that works by inhibiting FIB-1 translation, which is required for ribosome RNA transcription and maturation [15–17]. An independent *ncl-1* loss of function allele *(e1942)* also suppressed the developmental arrest of *ddx-52*(lf) (Figure S1A). Thus, *ncl-1*(*gc53*) behaves as a loss of function allele. *gc54* and *gc55* were identified as missense alleles of *ulp-4*. ULP-4 removes SUMO modifications from proteins and has been implicated in the mitochondrial unfolded response in aging and innate immunity [18–20] but has not previously been implicated in regulation of the translation machinery. *ulp-4(RNAi)* significantly suppressed the temperature-sensitive developmental arrest phenotype of *ddx-52*(lf) (Figure S1B). Thus, *ulp-4(gc54)* and *ulp-4*(*gc55*) behave as loss of function alleles. *gc58* was identified as a missense allele of *nol-10*. Another suppressor mutant was

found to have two missense mutations *gc63gc64* in the *aatf-1* gene. In yeast, orthologs of NOL-10 and AATF-1 (ENP2 and BFR2) physically interact with the DEAD-box RNA helicase Dbp4 to promote ribosome biogenesis [21]. Complete loss of function alleles *nol-10(ok2965)* and *aatf-1 (tm5125)* are lethal (https://www.wormbase.org/species/c_elegans/gene/). However, *nol-10*(*RNAi*) and *aatf-1*(RNAi) treated animals are viable and both act in a synergistic fashion with *ddx-52(gc51*) to arrest development even at 20°C (Figure S1C and S1D). Both RNAis also reduce the suppression of the temperature sensitive arrest of *ddx-52(gc51) by nol-10(gc58)* and by *aatf-1(gc63gc64)*, respectively (Figure S1C and S1D). Reducing the activity of these two genes in wild type animals by RNAi produced hypoxia resistance (Fig S1E and S1F). These data suggest that *gc58* is a gain of function mutation in NOL-10 and that *gc63 and/or gc64* is a gain of function mutation in AATF-1. Based on the molecular and genetic characterization of the suppressor mutations, the predicted effect of DDX-52 and the suppressor genes on ribosome biogenesis is shown in Figure 2C.

Suppressors restore hypoxic sensitivity to *ddx-52(lf)*

To test if the suppressors of temperature-induced arrest of *ddx-52*(lf) also suppressed its hypoxia resistance, we outcrossed suppressor alleles from our screen (except for *larp-1*) six times and then crossed them back to *ddx-52(lf)*. We used and outcrossed *larp-1(q783)* since it is more likely to be a complete loss of function allele than the two missense alleles identified from our screen. Both *ncl-1*(lf) and *larp-1*(lf) suppressed the hypoxia resistance of *ddx-52*(lf) (Figure 2D). The suppression of hypoxia resistance by *ncl-1*(lf) and *larp-1*(lf) was additive (Figure 2D). Two independent missense alleles in *ulp-4* and the gain of function allele of *aatf-1* also partially suppressed the hypoxia resistance of *ddx-52(lf)*; however, the apparent suppression by *nol-10*(*gc58*) did not reach statistical significance (Figure 2E and 2F). Therefore, all suppressors of the temperature-induced developmental defect, except perhaps *nol-10*(*gc58*), also suppressed hypoxia resistance of *ddx-52*(lf). Given that the mutations in *ncl-1, larp-1*, and *aatf-1*, each orthologs of known regulators of ribosome biogenesis, suppress the hypoxia resistant of a loss-of-function mutation of *ddx-52*, an ortholog of an established ribosome biogenesis gene, these results strongly support the hypothesis that ribosome biogenesis proteins are important regulators of hypoxic injury.

Translation machinery mutations cause hypoxia resistance

To determine the genetic identity of the other hypoxia resistance mutations from our first screen beside *ddx-52(gc51)*, we genetically mapped, sequenced, tested candidate mutations/RNAis, and thereby assigned four mutations to four other genes. This assignment revealed that each of the four genes encodes a protein known to promote protein synthesis (Table 1). We have previously shown that a missense reduction-of-function mutation in *rars-1* (encodes arginyl amino-acyl tRNA synthetase) caused hypoxia resistance and reduced protein synthesis [7]. Likewise, an RNAi screen for hypoxia resistance highlighted the importance of translation machinery in determining hypoxia sensitivity [6]. Thus, while it is not surprising to recover mutations in translation genes, the tremendous enrichment for genes involved in protein synthesis is striking and demonstrates that the translation machinery is critical to hypoxic sensitivity and likely the largest mutable functional class of genes to produce high level hypoxia resistance phenotypes, at least in *C. elegans.* A description of the

four hypoxia resistant genes and how the assignment was made of the hypoxia-resistance mutations to those genes follows.

The hypoxia resistance phenotype of *gc52* was assigned to a single nucleotide variation in the splice donor of the first intron of *tars-1* (encodes threonyl amino-acyl tRNA synthetase). Reducing the activity of TARS-1 in wild type worms by *tars-1*(RNAi) also caused hypoxia resistance (Figure S2A). Thus, we conclude that *tars-1(gc52)* behaves as a reduction-of-function allele. Given the location of the mutation in the splice donor site, we searched for additional *tars-1* mRNA isoforms in *tars-1(gc52)* animals but did not detect any by amplification of the transcripts and then visualization by agarose gel electrophoresis or by sequencing (Figure S2B and S2C), suggesting that *gc52* simply reduces the level of normal splicing thereby reducing TARS-1 protein as opposed to the production of a novel isoform of TARS-1. The hypoxia resistance phenotype of *gc59* was assigned to a 245 bp deletion in *xpo-3* (encodes an ortholog to exportin-T, a tRNA nuclear exporter) [22]. Two independent loss of function alleles of *xpo-3* (*ok1271* and *gk932618*)[11] also caused hypoxia resistance (Figure S2D). Thus, we conclude that *xpo-3*(*gc59*) behaves as a loss-of-function allele. The hypoxia resistance phenotype of *gc50* was assigned to a single nucleotide variation in the splicing donor of the first intron of *rtcb-1* (encodes a tRNA ligase [23]). RT-PCR from *rtcb-1(gc50)* animals demonstrated alternative splice isoforms as well as some migrating normally (Figure S2E). Therefore, *gc50* likely produces alternative protein isoforms and reduced the expression of full-length RTCB-1. An independent deletion and presumed null allele *rtcb-1(gk451)* [23] also caused hypoxia resistance and failed to complement *gc50* (Figure S2F). Thus, we conclude that *rtcb-1(gc50)* behaves as a loss-of-function allele. The hypoxia resistance of *gc60* was assigned to a nonsense mutation at Y464 in PEPT-1 (encodes an oligopeptide transporter [24–28]). An independent loss of function allele *(lg601)* [25] (Figure 3E) and *pept-1*(RNAi), as previously reported [6], (Figure S2G) also caused hypoxia resistance. *pept-1*(RNAi) has been previously shown to reduce global translation rate and *pept-1*(*lg601*) has reduced levels of essential amino acids for translation [28]. Thus, the hypoxia resistant mutants fell into three categories: 1) those that reduce availability/aminoacylation of tRNAs; 2) those that reduce ribosome biogenesis; 3) those that reduce raw amino acid substrates.

ddx-52(lf) suppressors restore hypoxic sensitivity to a subset of translation machinery mutants

We tested whether the hypoxia resistance of the other translation machinery mutants was also suppressed by suppressors of *ddx-52*(lf). Given that *larp-1, ncl-1, nol-10*, and *aatf-1* all have established functions in ribosome biogenesis, we expected that these mutants would not affect the hypoxia resistance of the tRNA pathway mutants. However surprisingly, the hypoxia resistance of *tars-1*(rf) was strongly suppressed by *larp-1*(lf) and *ncl-1*(lf) in an additive manner (Figure 3A). None of the other *ddx-52*(lf) suppressors significantly altered the hypoxia resistance of *tars-1*(rf) (Figure 3B). Similar to the *tars-1* mutant, the hypoxia resistance of *xpo-3(lf)* and *rtcb-1*(rf) were dependent on LARP-1 and NCL-1 (Figure 3C, 3D). As for *tars-1*(*gc52*), *ulp-4*(lf) did not suppress the hypoxia resistance of *rtcb-1*(rf) (Figure S3); however, unlike for the *tars-1 and rtcb-1* mutants, *ulp-4*(rf) did significantly suppress *xpo-3(gc59)*, albeit to a small degree (Figure 3C). Thus, the loss-of-function of

larp-1 and *ncl-1*, which normally function to inhibit ribosomal protein synthesis and ribosomal RNA transcription, respectively, suppressed the hypoxia resistance of all three tRNA pathway mutants as well as the *ddx-52* ribosome biogenesis mutant; however, the mutants in *nol-10* and *aatf-1*, which function downstream in ribosome maturation, did not suppress the tRNA pathway mutants. This broader suppression activity by the *larp-1* and *ncl-1* mutants could be explained by a model where increased ribosomal protein and RNA synthesis is able to overcome reduced translation substrates such as tRNAs and acylated tRNAs. Amino acids supplied by the oligopeptide transporter PEPT-1 would also be such a substrate. However, loss of LARP-1 and NCL-1 did not suppress the hypoxia resistance of *pept-1*(lf) (Figure 3E). This lack of suppression by the *larp-1*(lf) *ncl-1*(lf) double mutant of *pept-1*(lf) demonstrates a relative specificity for interaction with the tRNA biosynthesis pathway and argues against trivial explanations of how *larp-1*(lf) and *ncl-1*(lf) might suppress hypoxia resistance, such as the *larp-1*(lf) *ncl-1*(lf) animals just being sickly or sensitizing cells to hypoxia under any circumstance. We also tested whether suppressors of a distinct hypoxia resistance pathway [29–31], the insulin/IGF receptor pathway, might suppress *tars-1*(rf). However, a *daf-16*(lf) mutant, previously shown to suppress the strongly hypoxia resistant *daf-2*(rf) mutants and to suppress the enhancement of the long lifespan of *daf-2*(rf) by *pept-1*(*lg601*), did not suppress the hypoxia resistance of *tars-1*(rf) nor did it suppress that of *pept-1*(rf) (Figures 3A and S4). Thus, the hypoxia resistance of *tars-1*(rf) is not promiscuously suppressible. The common suppression of *ddx-52*(lf) and the tRNA pathway mutants by the *larp-1*(lf) *ncl-1*(lf) double mutant indicates that they produce hypoxia resistance by a common mechanism. If so, we would expect the hypoxia resistance of the mutations in the two genes to be non-additive. Indeed, the *ddx-52*(*gc51*); *tars-1*(*gc52*) double mutant was no more resistant than *tars-1*(*gc52*) alone (Figure 3F). As expected, the hypoxia resistance phenotypes of *tars-1*(*gc52*) and *xpo-3*(*gc59*) are not additive either (Figure 3G). However, the hypoxia resistance of *tars-1*(*gc52*) and *pept-1*(*lg601*) is additive (Figure 3H). These data argue that *larp-1, ncl-1, ddx-52*, and *tars-1* control hypoxic sensitivity by a common mechanism whereas *pept-1* acts through a distinct mechanism.

Protein synthesis of *tars-1* mutant fully restored by *larp-1 ncl-1* double mutant

To test whether the *tars-1* mutant did indeed have a reduced level of protein synthesis and whether the *larp-1*(lf) *ncl-1*(lf) mutant restored its translation activity, we performed polysome profiling of wild type animals and *tars-1(gc52)* animals and found that *tars-1*(rf) animals have reduced polysomes and monosomes, consistent with reduced translation (Figure 4A). The *tars-1*(rf); *larp-1*(lf) *ncl-1*(lf) triple mutant had a polysome profile intermediate between wild type and the *tars-1*(rf) single mutant. This argues that the combination of *larp-1*(lf) and *ncl-1*(lf) restores translation of the *tars-1* mutant towards normal. To measure this quantitatively, we assessed total protein synthesis using incorporation of ^{35}S-methionine-labelled bacteria into the mutant strains. As expected, *tars-1(rf)* animals have markedly reduced incorporation of ^{35}S compared to wild type worms (Figure 4B). However, *tars-1(rf);larp-1(lf) ncl-1(lf)* had ^{35}S incorporation levels similar to wild type worms, indicating that *larp-1 ncl*-1 fully suppresses the reduced translation levels of *tars-1*(rf). *pept-1*(lf) animals had reduced incorporation of ^{35}S similar in magnitude to that of *tars-1*(*gc52*), consistent with published studies reporting reduced protein synthesis in *pept-1*(lf) [28]. However, *larp-1*(lf) *ncl-1*(lf) did not restore the reduced protein synthesis

rates in the *pept-1(lf)* mutant (Figure 4B). Restoration of normal translation in the *tars-1* mutant but not in the *pept-1* mutant by *larp-1 ncl*-1 matches the suppression profiles for hypoxia resistance. This surprising ability of *larp-1*(lf) *ncl-1*(lf) to fully restore translation levels of the *tars-1(rf)* mutant suggests at least two novel non-mutually exclusive hypotheses: 1) reduction of *tars-1* function does not reduce translation simply by reducing the availability of threonyl-tRNAs; 2) increasing ribosome biogenesis can overcome reduced *tars-1* activity to restore normal translation rates.

tars-1 reduction-of-function results in a corresponding downregulation of ribosomal subunits and translation elongation factors

How are the regulators of ribosome biogenesis LARP-1 and NCL-1 able to increase translation to normal levels despite reduced TARS-1 activity? To define the *tars-1(rf)* proteome and how LARP-1 and NCL-1 might affect it, we analyzed the wild type, *larp-1*(lf) *ncl-1*(lf), and *tars-1*(rf) mutant proteomes in isolation and when combined. We first examined the effect that the fraction of threonine in each protein had on its synthesis rates. We expected that the synthesis rates of proteins with a higher fraction of threonines would be more greatly affected by reduced *tars-1* function. To test this hypothesis, we measured the rates of incorporation of heavy lysine into the proteomes of the various strains. To our surprise, threonine frequency in proteins had no correlation with heavy lysine incorporation rate in the *tars-1*(*gc52*) mutant nor in the *tars-1*(*gc52*);*larp-1*(lf) *ncl-1*(lf) suppressed mutant strain (Figure 5A and 5B). The lack of effect of threonine frequency on protein synthesis rate in the *tars-1* mutant is consistent with the hypothesis that reduction of *tars-1* function does not reduce translation simply by reducing the availability of threonyl-tRNAs.

We used tandem mass tag (TMT) and label-free quantification (LFQ) methods to measure what specific proteins were selectively affected in the mutant proteomes compared to wild type. 2385 proteins were identified in the TMT-labelled samples in all four strains and 2587 proteins in the LFQ samples. As expected TARS-1 protein was decreased in the *tars-1(gc52)* animals relative to wild type (TARS-1 abundance ratio in gc52/N2=0.22±0.07 in TMT, =0.20±0.03 in LFQ) (Data S1B, S1C). Likewise, LARP-1 was decreased in the *larp-1*(lf) *ncl-1*(lf) strain (*q783* gc53/N2=0.049±0.013 in TMT, =0.21±0.08 in LFQ) (Data S1D, S1E). NCL-1 was not detected in wild type or in any of the mutant strains. In the *tars-1(gc52);larp-1(q783) ncl-1(gc53)* triple mutant, the reduced levels of both TARS-1 and LARP-1 were maintained (TARS-1 – triple/N2=0.21±0.06 in TMT, =0.22±0.02 in LFQ; LARP-1 – triple/N2=0.077±0.014 in TMT, =0.19±0.08 in LFQ) (Data S1F, S1G). These data rule out restoration of TARS-1 protein levels as a trivial explanation for *larp-1*(lf) *ncl-1*(lf) suppression of *tars-1*(lf) mutant phenotypes.

To identify functional networks of proteins that might be responsible for the *tars-1* mutant phenotypes and their suppression by *larp-1*(lf) *ncl-1*(lf), STRING network analysis with Markov clustering [32] was performed on the sets of proteins significantly increased or decreased in each mutant strain relative to wild type in the TMT dataset (Data S2, Data S1G–S1M). In the *tars-1(gc52)* proteome, there were no large functional clusters (largest cluster=12) in the proteins with increased abundance (Data S1H). However, among the significantly decreased proteins in *tars-1(gc52)* (196 proteins total), the largest network

cluster (colored red) contained 52 proteins composed of translation machinery proteins (enrichment for GO:0006412 – translation $p = 1.2x10^{-24}$), including 33 of the 79 cytosolic ribosomal structural proteins and four of the six translation elongation factors (Data S2A, Data S1I). Interestingly, only two of the 33 subunits composing the 13 core translation initiation factors were in the downregulated set. Thus, reduction of function of *tars-1* produces a highly biased reduction in translation machinery proteins, specifically ribosomal subunits and elongation factors. Broadening the definition of cytosolic ribosomal proteins to include those annotated as functioning in ribosome maturation or biogenesis along with the structural subunits produced a set of 125 proteins detected in both the TMT and LFQ datasets. Remarkably, 93 of these proteins had decreased abundance in *tars-1*(*gc52*) in both the TMT and LFQ samples relative to wild type (Figure 5C, Data S1A); this decreased level of ribosomal-related proteins was highly significantly different from the proteome as a whole (Figure 5D). This indicates that there is a previously undescribed mechanism whereby the cell responds to reduced threonyl-tRNA synthetase activity or levels by downregulating ribosomal subunits. This also suggests the surprising possibility that the decreased translation rate observed in *tars-1*(*gc52*) is due to decreased ribosome levels and not to the actual reduction in TARS-1 enzymatic activity. This conclusion is consistent with the fact that the synthesis rates of proteins are not a function of their threonine content in the *tars-1*(rf) mutant (Figure 5A and 5B).

Not surprisingly given the known function of both NCL-1 and LARP-1 in negatively regulating ribosome biogenesis, the increased proteins in the *larp-1*(lf) *ncl-1*(lf) mutant were highly enriched in ribosome biogenesis proteins (enrichment for GO:0042254 – ribosome biogenesis $p = 3.1x10^{-28}$) (Data S1J). The largest STRING cluster (colored red) consisted of 77 proteins composed primarily of proteins annotated as promoting ribosome maturation and biogenesis (Data S2B, Data S1J); remarkably, this cluster contained 66% of the 116 proteins with significantly increased abundance. Among the proteins significantly decreased in the *larp-1*(lf) *ncl-1*(lf), the largest cluster (colored red, 36 out of 192 proteins) was composed mostly of mitochondrial electron transport subunits (Data S2C, Data S1K). Neither LARP-1 nor NCL-1 has previously been linked to regulation of the mitochondrial electron transport chain, ATP production, or redox state; our data suggests that a feedback mechanism may exist to coordinate the expression of ribosomal proteins with mitochondria and/or electron transport chain proteins. In the triple mutant, the effect of *larp-1*(lf) *ncl-1*(lf) on ribosome biogenesis was maintained with the largest cluster (colored red) in the significantly increased set containing many ribosome biogenesis factors (Data S2D, Data S1L). In the triple mutant decreased abundance set, the largest cluster (colored red, 36 out of 222 proteins) was the same as in the *tars-1* mutant, ribosome structural proteins (Data S2E, Data S1M); however, none of the translation elongation factors were significantly decreased in the triple mutant. The second largest cluster (colored green, 31 out of 222 proteins) was composed primarily of the mitochondrial electron transport chain proteins seen in the *larp-1*(lf) *ncl-1*(lf) suppressor strain. Overall, the proteome of the triple mutant consists of networks of differentially-expressed proteins already present in the *tars-1*(lf) and *larp-1*(lf) *ncl-1*(lf) strains. With the potentially important exception of the normalization of the elongation factor levels, there were no clear emergent networks or disruption of networks when the hypoxia resistant and reduced translation rate *tars-1*(lf) mutant and *larp-1*(lf)

ncl-1(lf) mutant were put together to produce a non-hypoxia resistant, normal translation rate strain. Likewise, the differentially-expressed proteome of the triple mutant correlated strongly and equally with that of both the *tars-1*(rf) mutant (R^2=0.48 and the *larp-1*(lf) *ncl-1*(lf) mutant (R^2=0.52) (Figure S5A, S5B). As expected, the differentially-expressed proteomes of the *tars-1*(rf) mutant and *larp-1*(lf) *ncl-1*(lf) mutant did not significantly correlate with each other (R^2=0.095) (Figure S5A).

Discussion

Through unbiased mutagenesis screening in *C. elegans*, we originally set out to discover genes that regulate survival after cellular hypoxic injury. Indeed, we identified five such genes that when mutated strongly protect from hypoxic injury. Each of these genes encodes a protein with an established role in protein synthesis in *C. elegans* and/or other organisms. Coupled with our previously published studies showing that reducing the function of many translation factors can produce hypoxia resistance [6–8], our data indicate that the translation machinery is a powerful regulator of hypoxic injury and should be examined as a therapeutic target for disease processes involving hypoxia, including stroke, myocardial infarction, and cancer. With translation factor knockdown or mutation, we have previously shown no correlation of the level of hypoxia resistance with oxygen consumption and have shown that knockdown of translation factors only after hypoxia during recovery reduces delayed hypoxic death [7, 8, 33]. These data are not consistent with the widely stated assumption that reduction of translation is hypoxia protective simply because it reduces oxygen consumption during the hypoxic insult [34–36]. However, what exactly is the underlying mechanism of hypoxia protection is still unclear. Our suppressors revealed at least two pathways whereby translation regulates hypoxic sensitivity: one controlled by LARP-1 and NCL-1 and the other by the oligopeptide transporter gene PEPT-1. The proteomics data show that the overwhelming effect of the *larp-1*(lf) *ncl-1*(lf) double mutant is to upregulate ribosome biogenesis. Thus, the RNA helicase gene *ddx-52* and the tRNA pathway genes, *tars-1, xpo-3*, and *rtcb-1*, all regulate translation and hypoxic sensitivity via a mechanism sensitive to ribosome biogenesis whereas the oligopeptide transporter gene *pept-1* does not, despite the established function of *pept-1* to promote protein synthesis. The nature of our suppressors and their proteomes suggests that ribosomes or something downstream of ribosomes promote hypoxic injury. A graphical summary of the data is provided in Figure 6.

Perhaps, the most surprising finding of our work is that the combination of the *larp-1* and *ncl-1* suppressor mutations could fully restore protein synthesis as measured by ^{35}S-methionine incorporation to an animal with reduced *tars-1* function. Regardless of how many ribosomes are available, tRNA is still needed for successful translation. In an otherwise wild type background, the *tars-1*(lf) mutant has a markedly reduced global translation, about a third of that in a strain with wild type *tars-1* (Figure 4B). The natural assumption is that this reduction in translation rate is due to reduced availability of threonyl-tRNA, which should cause pausing of translation at each threonine codon and slow protein synthesis, particularly proteins with high threonine content. However, this assumption is not supported by our SILAC incorporation data showing the rate of translation of individual proteins is unrelated to their threonine content (Figure 5A,5B). Rather, our data argue that

the translation machinery senses reduced threonyl-tRNA and lowers synthesis rates globally so that incorporation of threonine is no longer the rate-limiting step in translation. The combination of our genetic and proteomic data argues that the mechanism whereby the global translation rate is lowered is through *larp-1 ncl-1*-mediated reduction of certain ribosomal subunits and elongation factors. However, the details of this mechanism – how threonyl-tRNA levels are sensed and the nature of the regulatory feedback to reduce ribosomes and elongation factors slowing translation of proteins, regardless of threonine content, is unknown.

In eukaryotes, the mTOR pathway responds to amino acid deprivation by downregulating translation, in part by inhibiting ribosome biogenesis [37]. Recently, mammalian LARP1 has been shown to be a substrate of mTORCl; LARP1 phosphorylation by mTORCl relieves the inhibitory action of LARP1 on ribosomal protein synthesis [12]. Combining mTOR regulation of LARP1 with our genetic results, a reasonable hypothesis is that reduced TARS-1 activity inhibits mTOR thereby disinhibiting LARP-1, resulting in reduced ribosomal subunit synthesis. How TARS-1 activity might regulate mTOR is unknown. Notable here, *ncl-1*(lf) appears to further suppress the residual hypoxia resistance of the *tars-1*(*gc52*);*larp-1*(*q783*) double mutant (p=0.015, unpaired 2-tailed t-test). Thus, the hypoxia resistance of *tars-1*(lf) does not derive exclusively through LARP-1 activation. However, given that *ncl-1*(lf) also acts to disinhibit ribosome biogenesis [15], the *ncl-1*(lf) should suppress the reduced ribosomal subunit levels of *tars-1*(lf) and its hypoxia resistance, even if the primary effect of *tars-1*(lf) is LARP-1 activation. *larp-1*(lf) *ncl-1*(lf) also suppress *xpo-3*(lf) and *rtcb-1*(lf). *xpo-3* encodes exportin-T, which functions to transport tRNAs out of the nucleus [22]. *rtcb-1* encodes the only known *C. elegans* tRNA ligase, which splices the intron-containing tRNAs for alanine, leucine, isoleucine, and tyrosine [23, 38, 39]. Thus, unlike *xpo-3*(lf), which presumably reduces the levels of all tRNAs, *rtcb-1*(lf) should affect only this small subset. However like *tars-1*(*gc52*), the hypoxia resistance of both mutants is fully suppressed by *larp-1*(lf) *ncl-1*(lf). Thus, it will be important in future studies to determine whether the *rtcb-1* and *xpo-3* mutants similarly reduce ribosomal subunit levels as does the *tars-1* mutant and likewise for our previously isolated mutant for arginyl-tRNA synthetase [7]. This will allow us to determine whether the crosstalk between tRNAs and ribosome biogenesis is specific to TARS-1, to aminoacyl-tRNA synthetases, or extends more broadly.

In conclusion, we have discovered a regulatory interaction between threonyl-tRNA synthetase and ribosome biogenesis that regulates global translation and hypoxic sensitivity. The nature of this regulatory interaction is unknown. The most parsimonious interpretation of the genetics and proteomics data is that the reduction in *tars-1* activity reduces mRNA translation into proteins not directly by a loss of enzymatic activity, rather by an uncharacterized feedback mechanism to downregulate ribosomal subunits and translation elongation. Future work will determine whether this tRNA – ribosome/elongation factor crosstalk extends to other tRNA perturbations.

STAR Methods

RESOURCE AVAILABITY

CONTACT FOR REAGENT AND RESOURCE SHARING

Lead Contact: Further information and requests for resources and reagents should be directed to and will be fulfilled by the Lead Contact, C. Michael Crowder (cmc53@uw.edu).

Materials Availability: New mutant strains generated by mutagenesis in this work have been deposited in the *C. elegans* Genetics Center (CGC, University of Minnesota). Double and triple compound mutants and transgenic animals are available from the lead contact by request.

Data and Code Availability: The raw genomic sequence data from this study have been submitted to the NCBI BioProject (http://www.ncbi.nlm.nih.gov/bioproject) under accession number PRJNA555631. The raw proteomics data have been deposited in the ProteomeXchange Consortium via the PRIDE partner repository with the dataset identifier PXD017267.

EXPERIMENTAL MODEL AND SUBJECT DETAILS

***C. elegans* strains and maintenance:** Animals were maintained at 20°C on nematode growth media (NGM) plates seeded with *Escherichia coli* OP50. The N2 (Bristol) strain was the standard wild type strain from the *C. elegans* Genetics Center (CGC, University of Minnesota). Compound mutants were constructed using standard genetic techniques. Genotypes were confirmed by PCR amplification or by PCR followed by restriction digest. Strains generated and/or used in this work are listed in the Key Resource Table. Standard *C. elegans* nomenclature is used throughout [40].

METHOD DETAILS

Transgenesis: To generate strains with DDX-52::GFP extrachromosomal arrays, we PCR amplified from N2 genomic DNA a 4kb region upstream of the operon containing *ddx-52* using the following primers: 5'-gctaacaacttggaaatgaaataCCGGCTGGCCTAGAATATG-3' and 5'-atgccaaggaCATTCCTTTAAAAACGACAAATTGG-3'. We also amplified *ddx-52* from N2 genomic DNA using the following primers: 5'-taaaggaatgTCCTTGGCATTTAGAACC-3' and 5'-tggccaatcccggggatcctcTATATTCTTATTGTTCTTCTTGATCAAC-3'. Both PCR products were then assembled into pPD95.75 cut with HindIII /XbaI using NEBuilder® HiFi DNA Assembly Cloning Kit (New England Biolabs). The assembled plasmid was sequenced (Genewiz – https://www.genewiz.com/) and then microinjected into worms along with pRF4[*rol-6(su1006)*] as a co-injection marker.

RNAi: Feeding RNAi was performed as previously described [8]; however, LB was used instead of 2xYT and tetracycline was not used. The negative control (normal hypoxic sensitivity) for all RNAi experiments is feeding with the L4440 bacterial strain which is transformed with an empty vector expressing no double-stranded RNA [8].

Hypoxic death assays: Synchronized young adult worms were subjected to hypoxia as described previously except that hypoxic incubation temperature was 26.5°C [41]. Briefly, each plate of worms was washed into one 1.5 ml tube with 1 ml of M9 buffer (22 mM KH2PO4, 22 mM Na2HPO4, 85 mM NaCl, 1 mM MgSO4). Worms were allowed to settle by gravity, and 900 μl of M9 was removed. The tubes were then placed in the anaerobic chamber (Forma Scientific) at 26.5°C for the indicated incubation times. Typically for each strain in a trial, three plates of worms with approximately 30 worms/plate (each plate is treated as a technical replicate) were tested. Hypoxic incubations were varied according to the level of resistance of the strains tested. A non-hypoxia-resistant negative control and hypoxia resistant positive control were present in all trials for all hypoxia experiments excess those for additivity (Figure 3F–3H). The level of sensitivity of the strains, particularly the wild type strain, does vary from trial to trial, primarily as a function of small variations in oxygen concentration and temperature in the hypoxia chamber. Thus, statistics are always done against concurrent controls. Oxygen tension was always ≤ 0.3%. Following the hypoxic insult, worms were placed using glass Pasteur pipettes onto NGM plates spotted with OP50 bacteria and recovered at 20°C for 24 hours and then scored alive or dead. We have previously shown that animals recover to their full extent within the 24 hour recovery period [7, 30].

Developmental arrest assay: Gravid adult hermaphrodites were used for a two-hour egg lay at 20-22°C on NGM plates. Adult worms were then removed and the plates transferred to a 26°C incubator. After 72 hours, worms were visually scored for L1/L2 larval arrest or L1/L2 death versus normal development to the adult or L4 larval stage.

Forward genetic screens and mapping: Animals were mutagenized at the mid-L4 larval stage using N-ethyl-N-nitrosourea (ENU) at a concentration of 0.5 mM in M9 buffer for 4 hours at room temperature with gentle agitation. Mutagenized animals were then plated on NGM plates and were allowed to recover overnight at 20°C. For the hypoxia resistance screen, we screened ~ 20,000 haploid genomes. F2 animals that survived 24 hours of hypoxic exposure were picked and maintained. For suppressors of *ddx-52(gc51)* developmental arrest, we screened ~ 200,000 haploid genomes. F2 animals that developed to the L4 stage within 72 hours at 26°C were picked and maintained. Whole genome sequencing was performed by the University of Michigan sequencing core. Paired sequence reads were mapped to the *C. elegans* reference genome version WS230 (www.wormbase.org) using the short-read aligner BWA [42]. Single-nucleotide variants (SNVs) were identified and filtered with the help of the SAMtools toolbox [43]. Variant calls also present in the parental strain were eliminated, each SNV was annotated with a custom Perl script, and gene information downloaded from WormBase version WS230.

For the hypoxia resistance screen, single-nucleotide polymorphism mapping was performed using the polymorphic Hawaiian CB4856 strain and a set of 48 primer pairs distributed throughout the genome (eight per chromosome) that flank DraI restriction site polymorphisms [44]. Since the mutagenesis for the suppressor screen was performed on *ddx-52(gc51)* animals, we constructed a recombinant inbred strain for mapping (MC851 *gcIR1 (ddx-52(gc51)* I, N2>CB4856). Genomic mapping for causative mutations was done

by crossing mutant strains with the Hawaiian strain, which limited the causative mutation to one chromosome. For most mutant strains, genotyping assays were then designed to detect multiple single nucleotide variations (SNV) on the chromosome of the mutant strain. Mutant strains where then outcrossed with the N2 strain to separate the different SNV's into different lines. The different lines where then tested for the causative mutation phenotype. In most outcrossed strains in this study, the causative mutation was outcrossed from all neighboring SNV's that cause amino acid changes. Multiple approaches were used to reach a causative mutation gene assignment: outcrossing from neighboring mutations, outcrossing six times with the N2 strain, testing independent alleles of the same gene, genetic complementation and RNAi.

Polysome profiling: L4 stage worms were washed three times with cold M9 buffer supplemented with 1 mM cycloheximide and once with lysis Buffer without RNasin and PTE/DOC. Worms were then resuspended in 450µl of cold Lysis buffer (20mM Tris pH 8.5, 140 mM KCl, 1.5 mM MgCl2, 0.5 % Nonidet P40, 2% PTE (polyoxyethylene-10-tridecylether), 1% DOC (sodiumdeoxycholate monohydrate), 1mM DTT, 1mM cycloheximide, 0.4 U/µl RNasin (Sigma)). Worms were flash frozen in liquid N2 and then crushed with mortar and pestle precooled with liquid N2 (60 strokes with each pestle). Samples were then stored on ice for 40 minutes with vortexing every 10 minutes. Samples were then spun 10 minutes at 10,000x g at 4°C. Supernatant was collected and stored at −80°C. Samples were thawed and equal OD (A254) was brought to equal volume with lysis buffer and then layered on 10% to 50% (w/v) sucrose gradients. The gradients were centrifuged at 37,000 rpm for 2.5hrs at 4°C in a Beckman SW41Ti rotor, and fractionated by upward displacement through a Bio-Rad EM-1 UV monitor (Biorad) for continuous measurement of the absorbance at 254 nm using a Biocomp Gradient Station (Biocomp).

^{35}S methionine labeling: Gravid worms were washed and resuspended in 2 ml of M9 and then treated with 1ml Alkaline Hypochlorite Solution (per volume: 60% bleach and 40% 4M NaOH) for ~ 4 minutes. Eggs were washed with M9 and transferred to agarose plates seeded with OP50 bacteria. Agarose plates were prepared by mixing 975 ml H2O, 3 g NaCl and 17 g Agarose. The mixture was autoclaved, cooled and then supplemented with 1 ml of 1 M CaCl2, 1 ml of 5 mg/ml cholesterol in ethanol, 1 ml of 1 M MgSO4 and 25 ml of 1 M phosphate buffer pH=6.0. The resulting mix was then poured into 6 cm petri plates. OP50 was grown in LB in the presence or absence of L-[^{35}S]-Methionine (PerkinElmer). Worms were transferred from cold OP50 to hot OP50 plates by washing the worms off with M9. For protein extraction, L4 stage worms were pelleted, washed, and the pellet flash frozen in liquid nitrogen, thawed then resuspended in 200 µl of 1% SDS and boiled for 15 minutes with periodic vortexing. The tubes were centrifuged at 16,000 g, and the supernatant was removed into a new tube with equal volume ice cold 10% trichloroacetic acid and incubated for 1 hour on ice. The TCA precipitate was pelleted at 16,000 g and washed twice with ice-cold ethanol and allowed to air dry. The pellet was resuspended in 200 µl of 1% SDS, 0.1M Tris-HCl, pH=8.0 and boiled for 30 minutes with periodic vortexing. Upon cooling, aliquots were used for determination of [protein] (BCA protein assay kit, Thermo) and radioactivity incorporation by liquid scintillation (PerkinElmer tri-Carb 810TR).

Proteomics: Gravid worms were washed and resuspended in 2 ml of M9 and then treated with 1ml Alkaline Hypochlorite Solution (per volume: 60% bleach and 40% 4M NaOH) for ~ 4 minutes. Eggs were washed with M9 and transferred to Agarose plates seeded with ET505 bacteria (CGSC, Yale). ET505 is defective in the synthesis of Lysine. To grow ET505 we used lysine drop-out EZ rich defined medium (Teknova) supplemented with tetracycline (10 μg/ml) and 0.4 mM lysine. To label ET505 bacteria with heavy lysine, we grew it in the presence of 0.4 mM L-Lysine-2HCl, 13C6 (Thermo). Full labeling of ET505 was assessed by LC/MS/MS analysis of proteome digested with Endoproteinase LysC (New England Biolabs). Worms were transferred from light lysine to heavy lysine plates by washing the worms off with M9. For protein extraction, L4 stage worms were washed 2x with 100 mM Ammonium Bicarbonate and then resuspend in 8M Urea.

Samples were sonicated, and then TCEP (Tris(2-carboxyethyl)phosphine hydrochloride) was added to 5mM final concentration and incubated at room temp for 30 min. Iodoacetamide (IAA) was then added to 10 mM final concentration and incubated at room temp for 30 min. Samples were then diluted 10x with 100 mM Ammonium Bicarbonate. Protein concentration was quantified with BCA protein assay kit (Pierce). 100 μg of protein lysate was digested with 2 mg of LysC overnight at 37°C and then stored at −80°C.

Protein half-life measurements by SILAC labeling and LC-MS analysis: 100 μg of SILAC worm lysates were digested at 37°C by Lys-C (Promega, Wl) overnight, and desalted with C18 Sep-Pak solid phase extraction cartridges (Waters, Milford, MA). The digested samples were analyzed by a Thermo Easy-nanoLC coupled with Thermo Q-Exactive Plus Orbitrap mass spectrometer. Approximate 1 μg of sample was loaded onto an in-house fabricated 40 cm × 75 μm C18 column (5 μm diameter, 100 Å pore size MichromMagic beads), and separated with a 90 min 10–30% B gradient (flow rate : 300 nL/min, A: 0.1% formic acid in water, B: 0.1% formic acid in acetonitrile) at temperate of 40°C. A top 20 data-dependent acquisition method was applied for MS data acquisition using following parameters: full MS scan resolution 70 k, AGC target 1e6, maximum ion injection time 100 ms, scan range 400~2000 m/z; MS/MS scan resolution 17.5 k, AGC target 5e4, maximum ion injection time 100 ms, isolation window 1.6 m/z, HCD NCE 35, scan range 200~ 2000 m/z. Data dependent setting parameter settings were loop count 20, underfill ratio 1%, intensity threshold 5e3, dynamic exclusion 10 s. Two technical replicates were carried out for each sample.

The MS raw files were searched against a target-decoy proteome database of *C. elegans* downloaded from Uniprot (53758 entries including both targets and decoys) using Comet (version 2018.01) [45] with the following parameters: precursor peptide mass tolerance 20 ppm, allowing for 0, + 1, + 2, or +3 ^{13}C offsets; fragment ion mass tolerance 0.02 Da; static modification, carbamidomethylation of cysteine (57.0215 Da); variable modifications, methionine oxidation (15.9949 Da), lysine ^{13}C isotope labeling 6.020129 Da; digestion enzyme, Lys-C. Peptide spectra matches (PSMs) from two technical replicates were compiled by PeptideProphet, and filtered with 0.5% PSM false discovery rate. MasschroQ (version 2.2.12) was applied for retention time alignment of technical replicates and extraction of peak areas of precursor ions of light peptides and their co-eluting heavy counterparts [46]. For each PSM, the log transformed heavy labeling fraction (LTHLF),

express as -In(1-F_H), where F_H=heavy peak area/(light peak area + heavy peak area) was calculated [47]. Within each biological replicate, the LTHLF measured for PSMs belonging to the same protein were grouped, and the median LTHLF after outlier removal was assigned as the LTHLF for this protein at specific time point. The protein turnover rate was estimated from the slope of linear regression of LTHLF versus SILAC labeling time (0 hr, 12 hr, 24 hr), and the results were filtered by correlation coefficient threshold of 0.9. The protein half-life was calculated by Ln2 divided by the slope of linear regression.

Label-free quantification (LFQ) of *C. elegans* strains: Worm lysates were digested by LysC, desalted and analyzed by nanoLC-MS with the same methods as described for the SILAC labeled samples. The MS data files were also searched against the target-decoy proteome database of *C. elegans* by Comet with the same parameters except that no variable modification was set for lysine. Peptide spectra matches (PSMs) from two technical replicates were compiled by PeptideProphet and filtered with 0.5% PSM false discovery rate. MasschroQ was employed to conduct LC retention time alignment and peak area extraction for all the identified peptides. Within each biological replicate, technical replicates from LC-MS runs of all four strains were grouped for retention time alignment. The peak areas under curves from extracted ion chromatograms were integrated for all input PSMs with 20 ppm mass tolerance of precursor ion. Within each biological replicate, the output peak area values from two technical replicates of each strain were averaged and converted to $\log_2$(mutant/WT) for each PSM. All the measured $\log_2$ ratios from PSMs belonging to one protein were grouped, and the median ratio after outlier rejection was assigned as the protein expression ratio measured for this biological replicate. Discrepancy of protein lysate amount used for digestion and instrument performance variation were normalized by the median $\log_2$(mutant/WT) ratio of all quantified proteins within each biological replicate.

TMT quantification of *C. elegans* strains: For samples used for TMT quantitation, 100 μg of protein lysates were reduced with 10 mM TCEP at 30°C for 30 min and then alkylated with 15 mM IAA at room temperature in dark for 30 min. Lysates were diluted 5 times using 100 mM Tris-HCl (pH 7.6) and then 2.5 μg trypsin (Promega, WI) was added. The mixture was incubated for digestion at 37°C overnight. Digests were acidified and desalted using the same procedures as described above. The eluant was dried with speed vacuum and then reconstituted in 20 μL 50 mM HEPES buffer (pH 8.5). Four TMT labels (126, 128, 129, and 131, 800 μg each) from a TMT 6-plex kit (ThermoFisher) were dissolved in 40 μL anhydrous ACN. 100 μg TMT label was added to each digest at a TMT label-to-peptide ratio of 1:1. The TMT-digest mixture was incubated at room temperature for 1 h, and the labeling reaction was quenched by addition of 5% hydroxylamine to a final concentration of 0.4%. The labeling mixture was speed vacuumed to dryness and reconstituted in 0.1% FA and stored at −80°C for later LC/MS measurements. For LC/MS analysis of TMT labeled peptides, the same instrumental parameters were applied with following exceptions: 4-hr 10-30% B LC gradient; MS2 on the top 10 intense precursor ions; and fixed first mass at 100 m/z. Comet-based protein identifications with the same search parameters described above were used except that fixed TMT modification of peptide N-termini and lysines of 229.162932 Da and digestion enzyme of trypsin were applied. Only those proteins that were

identified with minimal two unique peptides and FDR < 1% were selected for quantifications. Relative abundances of proteins were calculated based on the mean values of isotope impurity-corrected reporter ion intensities (I126, I128, I129, and I131) of all peptides using Libra module implemented in the Trans-Proteomic Pipeline [48].

QUANTIFICATION AND STATISTICAL ANALYSIS—For developmental arrest and hypoxic death assays, a minimum of three technical replicates with at least 30 animals/replicate were pooled for each biological replicate. The number of biological replicates is noted in the figure legends. Biological replicates were expressed as mean ± sem. Statistical comparisons were by two-tailed unpaired t-test with significance set at $p < 0.05$.

For both TMT and label-free quantitation, protein intensity ratios of mutant/WT were Log2 transformed and then median-center normalized for each biological replicate. Data over 3 or more biological replicates were averaged with student's t-test confidence interval calculated at 95% confidence level. Proteins with lower bound of $\log_2$(mutant/WT) ratio greater than 0.5 were considered significantly upregulated, while proteins with upper bound of $\log_2$(mutant/WT) ratio less than −0.5 were considered significantly down-regulated.

Supplementary Material

Refer to Web version on PubMed Central for supplementary material.

Acknowledgments:

We thank Tom Tompkins for his excellent technical contributions to this work. We also thank Ghassan Salloum, who helped design the Alexa skill for recording verbal scoring of phenotypes. The work was supported by NIH grants - 1R01NS109088 (OAI, CMC), 1R01NS100350 (CMC), 1R01GM129034 (MVG), R37CA230617 (ACH), R01DK119270 (ACH); 5R01GM086688 (JEB), 1R01HL144778 (JEB)

References

1. Uniacke J, Holterman CE, Lachance G, Franovic A, Jacob MD, Fabian MR, Payette J, Holcik M, Pause A, and Lee S (2012). An oxygen-regulated switch in the protein synthesis machinery. Nature 486, 126–129. [PubMed: 22678294]
2. Spriggs KA, Bushell M, and Willis AE (2010). Translational regulation of gene expression during conditions of cell stress. Mol Cell 40, 228–237. [PubMed: 20965418]
3. Romero-Ruiz A, Bautista L, Navarro V, Heras-Garvin A, March-Diaz R, Castellano A, Gomez-Diaz R, Castro MJ, Berra E, Lopez-Barneo J, et al. (2012). Prolyl hydroxylase-dependent modulation of eukaryotic elongation factor 2 activity and protein translation under acute hypoxia. J Biol Chem 287, 9651–9658. [PubMed: 22308030]
4. Robichaud N, and Sonenberg N (2017). Translational control and the cancer cell response to stress. Curr Opin Cell Biol 45, 102–109. [PubMed: 28582681]
5. Andreev DE, O'Connor PB, Zhdanov AV, Dmitriev RI, Shatsky IN, Papkovsky DB, and Baranov PV (2015). Oxygen and glucose deprivation induces widespread alterations in mRNA translation within 20 minutes. Genome Biol 16, 90. [PubMed: 25943107]
6. Mabon ME, Mao X, Jiao Y, Scott BA, and Crowder CM (2009). Systematic identification of gene activities promoting hypoxic death. Genetics 181, 483–496. [PubMed: 19047414]
7. Anderson LL, Mao X, Scott BA, and Crowder CM (2009). Survival from hypoxia in C. elegans by inactivation of aminoacyl-tRNA synthetases. Science 323, 630–633. [PubMed: 19179530]

8. Scott B, Sun CL, Mao X, Yu C, Vohra BP, Milbrandt J, and Crowder CM (2013). Role of oxygen consumption in hypoxia protection by translation factor depletion. J Exp Biol 216, 2283–2292. [PubMed: 23531825]

9. Khoshnevis S, Askenasy I, Johnson MC, Dattolo MD, Young-Erdos CL, Stroupe ME, and Karbstein K (2016). The DEAD-box Protein Rok1 Orchestrates 40S and 60S Ribosome Assembly by Promoting the Release of Rrp5 from Pre-40S Ribosomes to Allow for 60S Maturation. PLoS Biol 14, e1002480. [PubMed: 27280440]

10. Venema J, Bousquet-Antonelli C, Gelugne JP, Caizergues-Ferrer M, and Tollervey D (1997). Rok1p is a putative RNA helicase required for rRNA processing. Mol Cell Biol 17, 3398–3407. [PubMed: 9154839]

11. Thompson O, Edgley M, Strasbourger P, Flibotte S, Ewing B, Adair R, Au V, Chaudry I, Fernando L, Hutter H, et al. (2013). The Million Mutation Project: A new approach to genetics in Caenorhabditis elegans. Genome Res.

12. Hong S, Freeberg MA, Han T, Kamath A, Yao Y, Fukuda T, Suzuki T, Kim JK, and Inoki K (2017). LARP1 functions as a molecular switch for mTORC1-mediated translation of an essential class of mRNAs. eLife 6.

13. Lahr RM, Fonseca BD, Ciotti GE, Al-Ashtal HA, Jia JJ, Niklaus MR, Blagden SP, Alain T, and Berman AJ (2017). La-related protein 1 (LARP1) binds the mRNA cap, blocking eIF4F assembly on TOP mRNAs. eLife 6.

14. Philippe L, Vasseur J-J, Debart F, and Thoreen CC (2018). La-related protein 1 (LARP1) repression of TOP mRNA translation is mediated through its cap-binding domain and controlled by an adjacent regulatory region. Nucleic acids research 46, 1457–1469. [PubMed: 29244122]

15. Yi YH, Ma TH, Lee LW, Chiou PT, Chen PH, Lee CM, Chu YD, Yu H, Hsiung KC, Tsai YT, et al. (2015). A Genetic Cascade of let-7-ncl-1-fib-1 Modulates Nucleolar Size and rRNA Pool in Caenorhabditis elegans. PLoS Genet 11, e1005580. [PubMed: 26492166]

16. lyer-Bierhoff A, Krogh N, Tessarz P, Ruppert T, Nielsen H, and Grummt I (2018). SIRT7-Dependent Deacetylation of Fibrillarin Controls Histone H2A Methylation and rRNA Synthesis during the Cell Cycle. Cell reports 25, 2946–2954 e2945. [PubMed: 30540930]

17. Tessarz P, Santos-Rosa H, Robson SC, Sylvestersen KB, Nelson CJ, Nielsen ML, and Kouzarides T (2014). Glutamine methylation in histone H2A is an RNA-polymerase-I-dedicated modification. Nature 505, 564–568. [PubMed: 24352239]

18. Gao K, Li Y, Hu S, and Liu Y (2019). SUMO peptidase ULP-4 regulates mitochondrial UPR-mediated innate immunity and lifespan extension. eLife 8.

19. Sapir A, Tsur A, Koorman T, Ching K, Mishra P, Bardenheier A, Podolsky L, Bening-Abu-Shach U, Boxem M, Chou TF, et al. (2014). Controlled sumoylation of the mevalonate pathway enzyme HMGS-1 regulates metabolism during aging. Proc Natl Acad Sci U S A 111, E3880–3889. [PubMed: 25187565]

20. Pelisch F, Sonneville R, Pourkarimi E, Agostinho A, Blow JJ, Gartner A, and Hay RT (2014). Dynamic SUMO modification regulates mitotic chromosome assembly and cell cycle progression in Caenorhabditis elegans. Nature communications 5, 5485.

21. Soltanieh S, Lapensee M, and Dragon F (2014). Nucleolar proteins Bfr2 and Enp2 interact with DEAD-box RNA helicase Dbp4 in two different complexes. Nucleic Acids Res 42, 3194–3206. [PubMed: 24357410]

22. Gupta A, Kailasam S, and Bansal M (2016). Insights into the Structural Dynamics of Nucleocytoplasmic Transport of tRNA by Exportin-t. Biophysical Journal 110, 1264–1279. [PubMed: 27028637]

23. Kosmaczewski SG, Edwards TJ, Han SM, Eckwahl MJ, Meyer BI, Peach S, Hesselberth JR, Wolin SL, and Hammarlund M (2014). The RtcB RNA ligase is an essential component of the metazoan unfolded protein response. EMBO Rep 15, 1278–1285. [PubMed: 25366321]

24. Fei YJ, Fujita T, Lapp DF, Ganapathy V, and Leibach FH (1998). Two oligopeptide transporters from Caenorhabditis elegans: molecular cloning and functional expression. Biochem J 332 (Pt 2), 565–572. [PubMed: 9601088]

25. Meissner B, Boll M, Daniel H, and Baumeister R (2004). Deletion of the intestinal peptide transporter affects insulin and TOR signaling in Caenorhabditis elegans. J Biol Chem 279, 36739–36745. [PubMed: 15155758]
26. Spanier B, Rubio-Aliaga I, Hu H, and Daniel H (2010). Altered signalling from germline to intestine pushes daf-2;pept-1 Caenorhabditis elegans into extreme longevity. Aging Cell 9, 636–646. [PubMed: 20550516]
27. Benner J, Daniel H, and Spanier B (2011). A glutathione peroxidase, intracellular peptidases and the TOR complexes regulate peptide transporter PEPT-1 in C. elegans. PLoS One 6, e25624. [PubMed: 21980510]
28. Geillinger KE, Kuhlmann K, Eisenacher M, Giesbertz P, Meyer HE, Daniel H, and Spanier B (2014). Intestinal amino acid availability via PEPT-1 affects TORC1/2 signaling and the unfolded protein response. J Proteome Res 13, 3685–3692. [PubMed: 24999909]
29. Mabon ME, Scott BA, and Crowder CM (2009). Divergent mechanisms controlling hypoxic sensitivity and lifespan by the DAF-2/insulin/IGF-receptor pathway. PLoS One 4, e7937. [PubMed: 19936206]
30. Scott BA, Avidan MS, and Crowder CM (2002). Regulation of hypoxic death in C. elegans by the insulin/IGF receptor homolog DAF-2. Science 296, 2388–2391. [PubMed: 12065745]
31. Mendenhall AR, LaRue B, and Padilla PA (2006). Glyceraldehyde-3-phosphate dehydrogenase mediates anoxia response and survival in Caenorhabditis elegans. Genetics 174, 1173–1187. [PubMed: 16980394]
32. Szklarczyk D, Gable AL, Lyon D, Junge A, Wyder S, Huerta-Cepas J, Simonovic M, Doncheva NT, Morris JH, Bork P, et al. (2019). STRING v11: protein-protein association networks with increased coverage, supporting functional discovery in genome-wide experimental datasets. Nucleic Acids Res 47, D607–d613. [PubMed: 30476243]
33. Sun CL, Kim E, and Crowder CM (2014). Delayed innocent bystander cell death following hypoxia in Caenorhabditis elegans. Cell Death Differ 21, 557–567. [PubMed: 24317200]
34. Wheaton WW, and Chandel NS (2011). Hypoxia. 2. Hypoxia regulates cellular metabolism. Am J Physiol Cell Physiol 300, C385–393. [PubMed: 21123733]
35. Storey KB, and Storey JM (2010). Metabolic rate depression: the biochemistry of mammalian hibernation. Adv Clin Chem 52, 77–108. [PubMed: 21275340]
36. Fahling M (2009). Surviving hypoxia by modulation of mRNA translation rate. J Cell Mol Med 13, 2770–2779. [PubMed: 19674191]
37. Iadevaia V, Liu R, and Proud CG (2014). mTORC1 signaling controls multiple steps in ribosome biogenesis. Seminars in Cell & Developmental Biology 36, 113–120. [PubMed: 25148809]
38. Chan PP, and Lowe TM (2009). GtRNAdb: a database of transfer RNA genes detected in genomic sequence. Nucleic acids research 37, D93–D97. [PubMed: 18984615]
39. Ray A, Zhang S, Rentas C, Caldwell KA, and Caldwell GA (2014). RTCB-1 mediates neuroprotection via XBP-1 mRNA splicing in the unfolded protein response pathway. J Neurosci 34, 16076–16085. [PubMed: 25429148]
40. Tuli MA, Daul A, and Schedl T (2018). Caenorhabditis nomenclature. WormBook 2018, 1–14.
41. Mao XR, and Crowder CM (2010). Protein misfolding induces hypoxic preconditioning via a subset of the unfolded protein response machinery. Mol Cell Biol 30, 5033–5042. [PubMed: 20733002]
42. Li H, and Durbin R (2010). Fast and accurate long-read alignment with Burrows-Wheeler transform. Bioinformatics (Oxford, England) 26, 589–595.
43. Li H, Handsaker B, Wysoker A, Fennell T, Ruan J, Homer N, Marth G, Abecasis G, Durbin R, and Genome Project Data Processing, S. (2009). The Sequence Alignment/Map format and SAMtools. Bioinformatics (Oxford, England) 25, 2078–2079.
44. Davis MW, Hammarlund M, Harrach T, Hullett P, Olsen S, and Jorgensen EM (2005). Rapid single nucleotide polymorphism mapping in C. elegans. BMC Genomics 6, 118–128. [PubMed: 16156901]
45. Eng JK, Hoopmann MR, Jahan TA, Egertson JD, Noble WS, and MacCoss MJ (2015). A deeper look into Comet--implementation and features. J Am Soc Mass Spectrom 26, 1865–1874. [PubMed: 26115965]

46. Valot B, Langella O, Nano E, and Zivy M (2011). MassChroQ: a versatile tool for mass spectrometry quantification. Proteomics 11, 3572–3577. [PubMed: 21751374]

47. Visscher M, De Henau S, Wildschut MHE, van Es RM, Dhondt I, Michels H, Kemmeren P, Nollen EA, Braeckman BP, Burgering BMT, et al. (2016). Proteome-wide Changes in Protein Turnover Rates in C. elegans Models of Longevity and Age-Related Disease. Cell reports 16, 3041–3051. [PubMed: 27626671]

48. Deutsch EW, Mendoza L, Shteynberg D, Farrah T, Lam H, Tasman N, Sun Z, Nilsson E, Pratt B, Prazen B, et al. (2010). A guided tour of the Trans-Proteomic Pipeline. Proteomics 10, 1150–1159. [PubMed: 20101611]

Highlights

- Enhanced ribosome biogenesis restores translation despite reduced tRNA biogenesis
- Reduced tRNA biogenesis can selectively reduce ribosomal proteins
- This feedback mechanism controls both protein synthesis and hypoxic sensitivity
- The translation machinery is crucial to hypoxic sensitivity

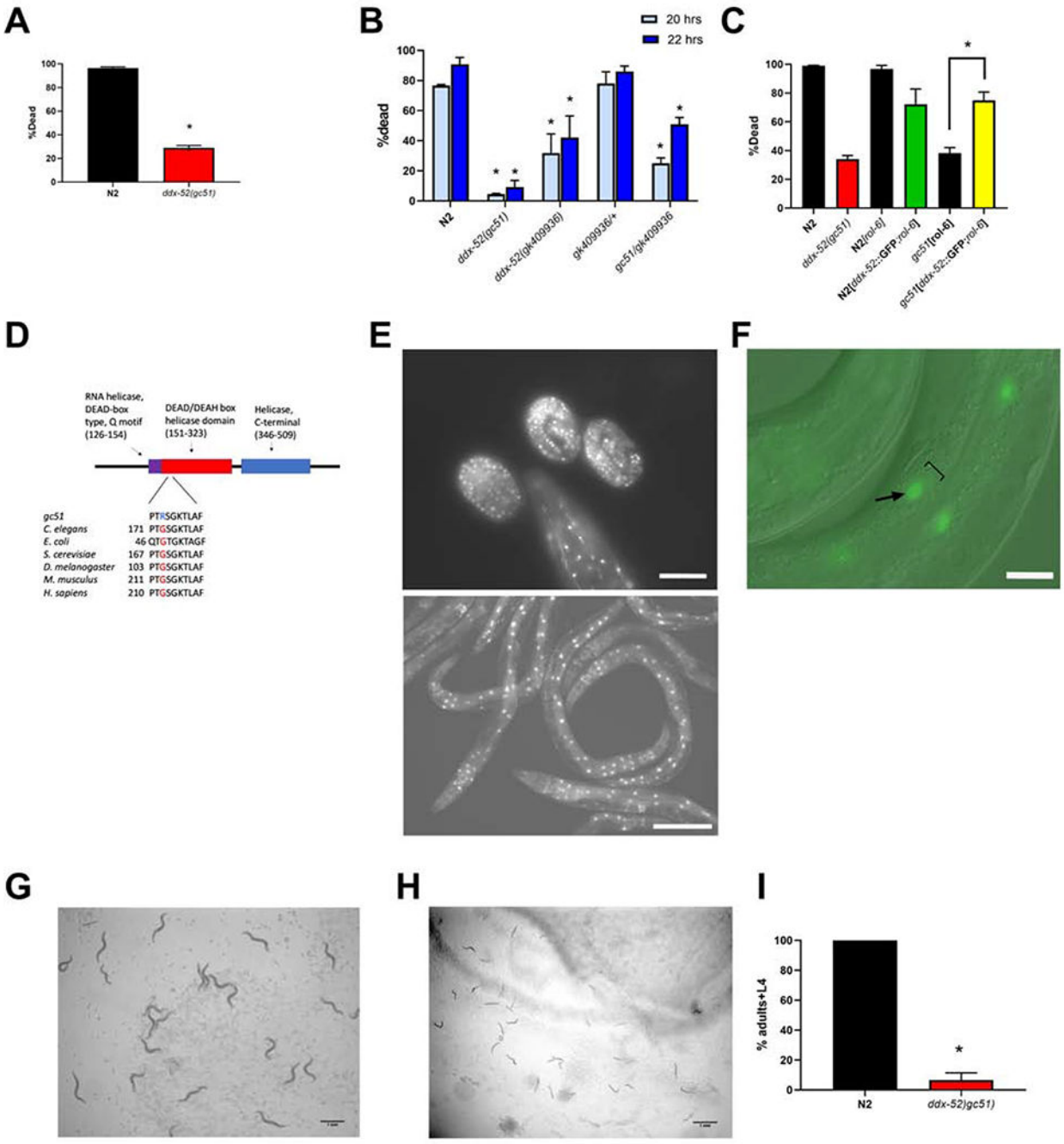

Figure 1. DDX-52 is an RNA helicase required for hypoxic death and for development at high temperature.

Different hypoxic incubation times are used based on the level of killing of the wild type strain N2 and the degree of resistance of the strains being tested. (A) *ddx-52*(*gc51*) causes hypoxia resistance. Fraction dead after a 24 hour recovery from a 24 hour hypoxic incubation. All data are mean +/− s.e.m. N=40 independent trials for both N2 and *ddx-52(gc51)*.). * $p < 0.01$ versus N2, 2-sided unpaired t-test. (B) Complementation testing with two *ddx-52* alleles. % dead after 24 hour recovery from a 20 or 22 hour hypoxic incubation. Data are mean % dead +/− s.e.m N=3 for all strains. * $p < 0.01$ versus N2, 2-

sided unpaired t-test. (C) Transformation rescue of *gc51* hypoxia resistance by expression of wild type ddx-52. Death after 24 hour recovery from 24 hours hypoxia for strains with and without extrachromosomal copy of wild type *ddx-52* or the transformation marker *rol-6*. N=3. * p<0.01, 2-sided unpaired t-test. (C) DDX-52 protein domains. Protein domain prediction (InterPro). Image drawn to scale. Alignment of the ATP binding motif of DDX-52 with the closest ortholog of the indicated species (BLAST). Numbers indicate amino acid positions. (E) DDX-52::GFP is ubiquitously expressed in a nuclear pattern in embryos (above – scale bar=50 μm) and adults (below - scale bar=100 μm). (F) DDX-52::GFP nucleolar expression. Merged DIC, fluorescent channel image. Nucleus indicated by bracket; nucleolus by arrow. DDX-52::GFP expression in the nucleolus. Scale bar=20 μm (G, H, I) *ddx-52(gc51)* causes developmental arrest at 26°C. Newly laid eggs were incubated at 26°C for 72 hours. N2 (**G**) and *ddx-52(gc51)* (**H**) animals were then visually scored for the fraction of animals normally developing to the L4 larval or adult stage (**I**). See Table S1. Scale bars = 1mm. Data are mean % adults/L4 +/− s.e.m (N=22 trials, >100 animals/trial). * p<0.01, 2-sided unpaired t-test

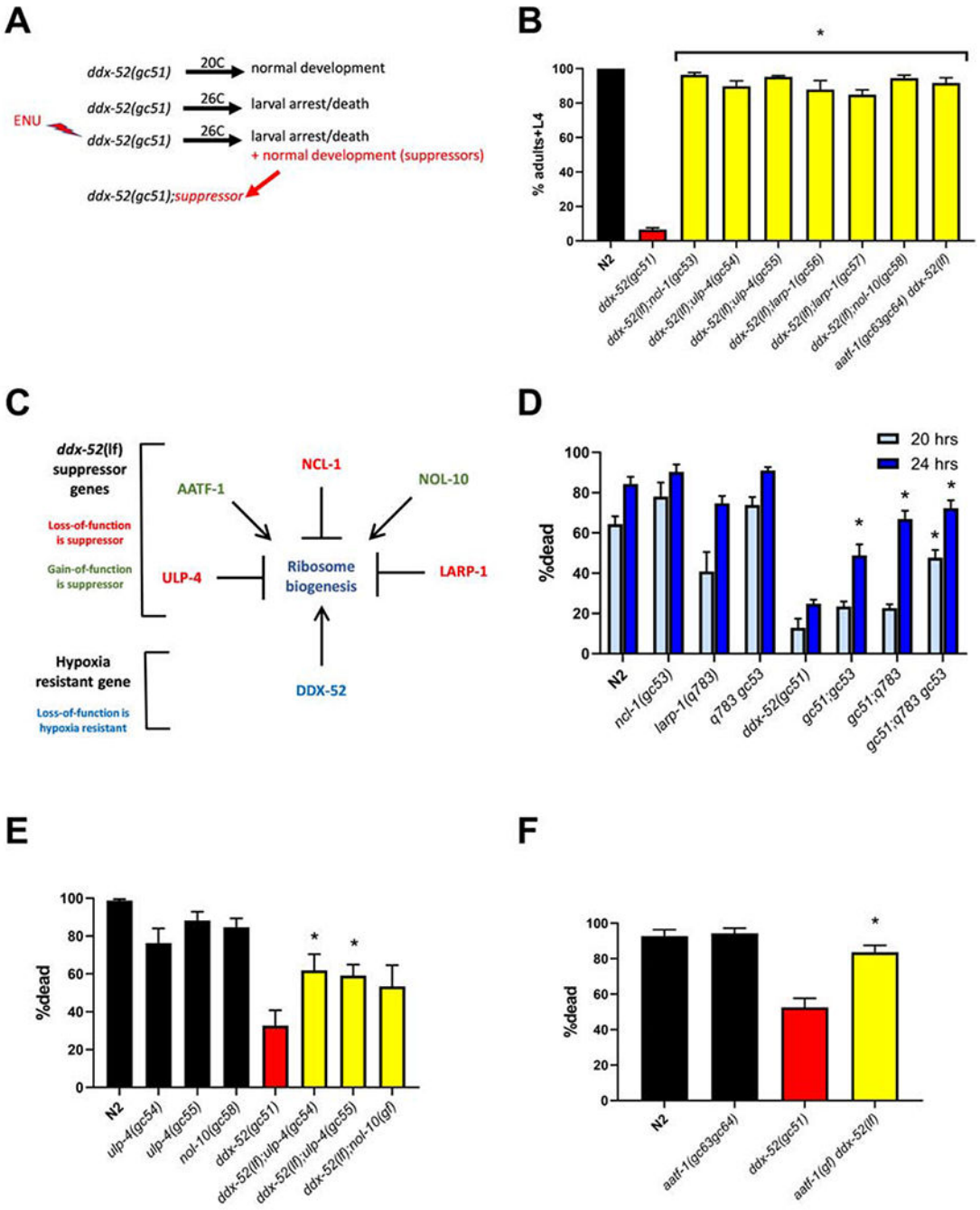

Figure 2. Isolation of genetic suppressors of *ddx-52(gc51)*.

(A) Suppressor screen strategy. (B) Isolated suppressor strains. Animals with the noted genotypes were grown at 26°C for 72 hours and number of animals developing into adults/L4 larvae was scored. Data are mean +/− s.e.m (N≥3). *p<0.01 versus *ddx-52(gc51)*, unpaired 2 sided t-test. (C) Model for predicted effect of DDX-52 and suppressor gene products, NCL-1, LARP-1, ULP-4, AATF-1 and NOL-10 on ribosome biogenesis. (D-F) Effect of suppressors on *ddx-52(gc51)* hypoxia resistance. % death after recovery from 20 or

24 hours of hypoxia (**E,F** 20 hours hypoxia). Data are mean +/− s.e.m (N≥3). *p<0.05 *vs ddx-52(gc51)* at same incubation time, 2-sided unpaired t-test. See Figure S1, Table S2.

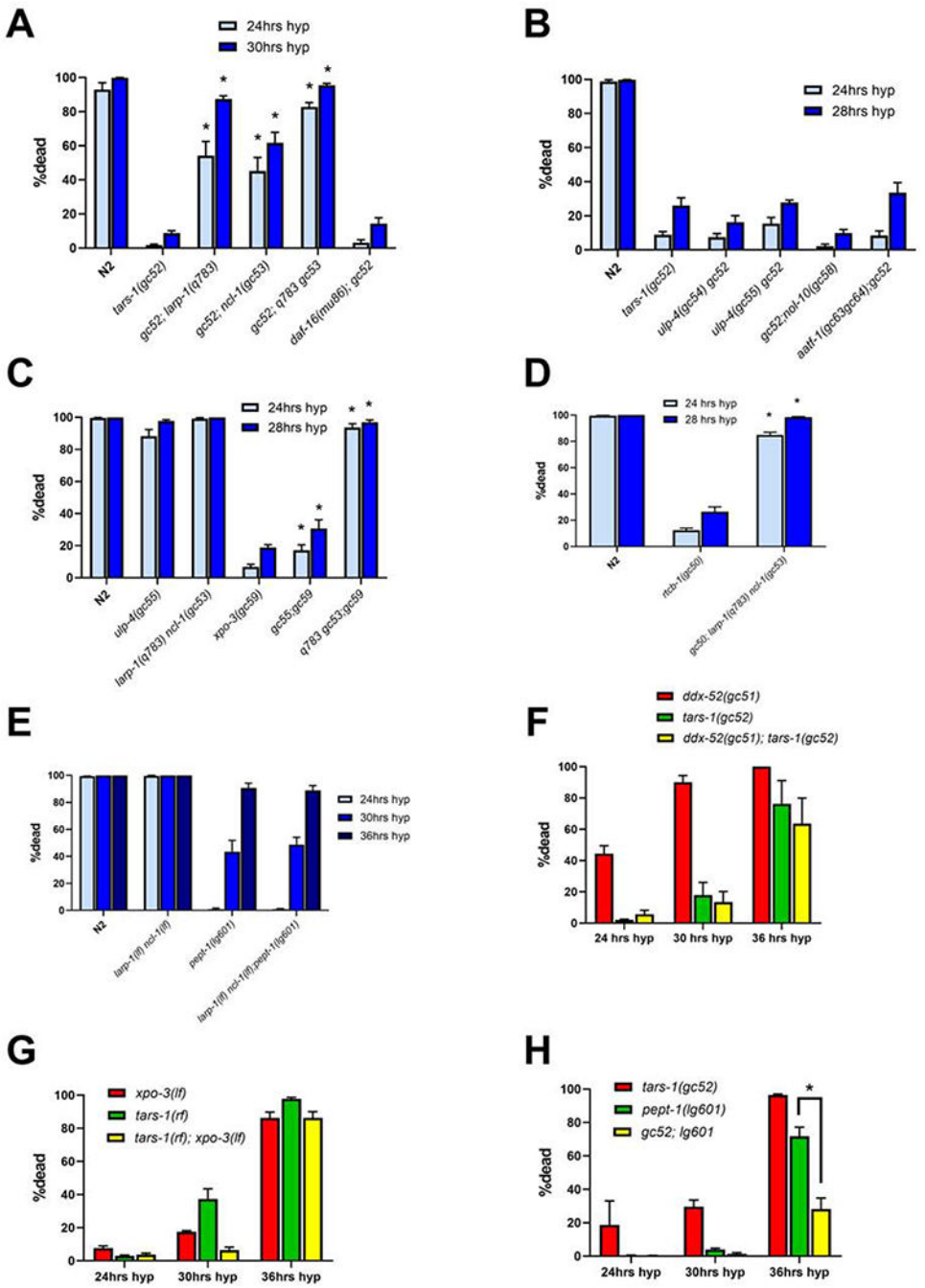

Figure 3. Genetic interaction of hypoxia resistant mutants with suppressors and each other.

% death after 24-hour recovery from the noted hypoxic incubation times. Data are mean +/− s.e.m (N≥3). * $p<0.05$ versus single hypoxia resistant mutant, 2-sided unpaired t-test (A) effect of *larp-1*(lf), *ncl-1*(lf) and the insulin receptor suppressor *daf-16*(lf) on hypoxia resistance of *tars-1*(rf). (B) effect of *ulp-4*(rf), *nol-10*(gf) and *aatf-1*(gf) on *tars-1*(rf). (C) effect of *larp-1*(lf) *ncl-1*(lf) and *ulp-4*(rf) on *xpo-3*(lf). (D) effect of *larp-1*(lf) *ncl-1*(lf) on *rtcb-1*(rf). (E) effect of *larp-1*(lf) *ncl-1*(lf) on *pept-1*(lf). (F) lack of additivity of the hypoxia

resistance of *tars-1*(rf) and *ddx-52*(lf) (G) lack of additivity of *tars-1*(rf) and *xpo-3*(lf) (H) additivity of *tars-1*(rf) and *pept-1*(lf). See Figure S2, S3, S4.

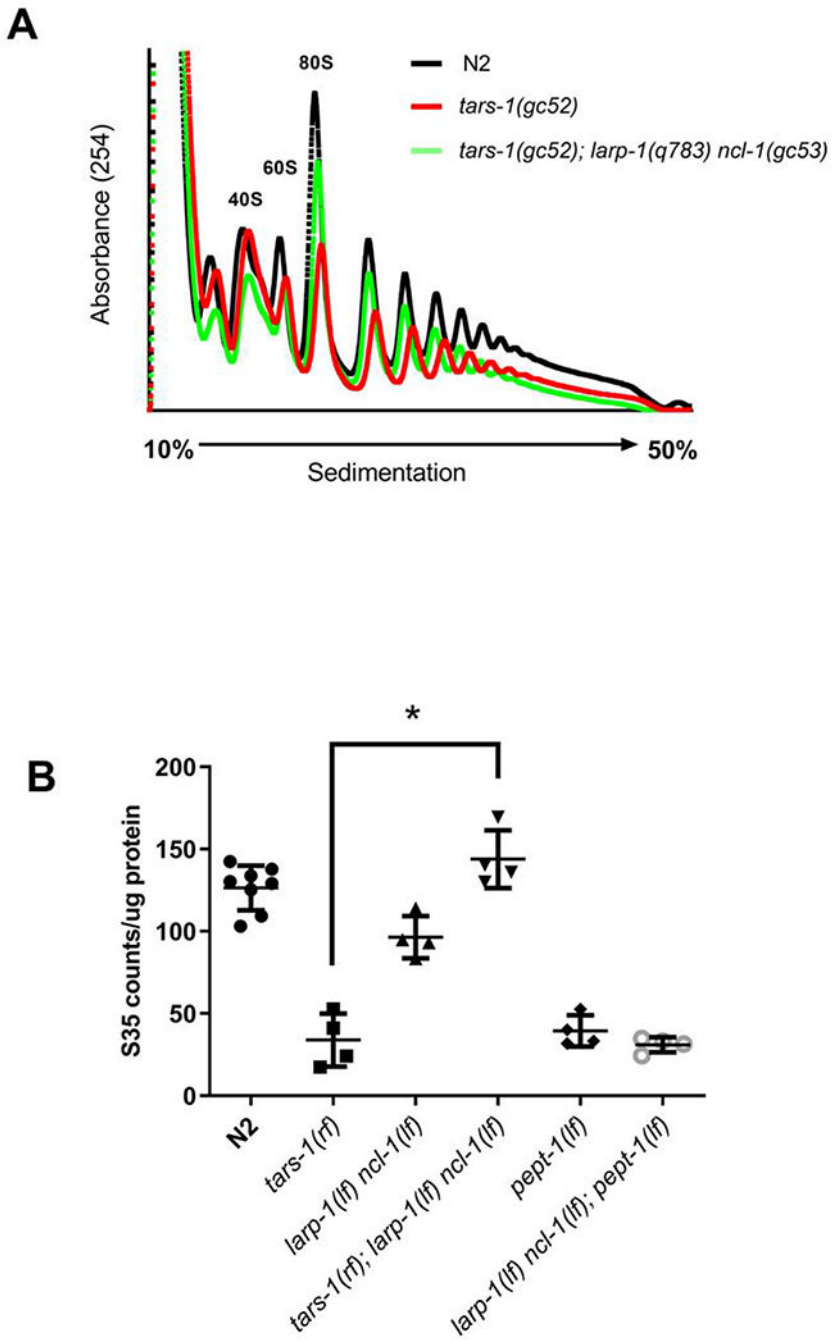

Figure 4. Restoration of translation in *tars-1*(rf) but not in *pept-1*(lf) by *larp-1*(lf) *ncl-1*(lf).

(A) Polysome profiles of N2, *tars-1(gc52)*, and *tars-1(gc52); larp-1(q783) ncl-1(gc53)*. Representative traces are shown (N=4). (B) *larp-1*(lf) *ncl-1*(lf) restore wild type levels of incorporation of ^{35}S methionine in *tars-1(rf)* but not in *pept-1(lf)* Wild type (N2), *tars-1(gc52), larp-1(q783) ncl-1(gc53), tars-1(gc52); larp-1(q783) ncl-1(gc53), pept-1(Ig601)* and *larp-1(q783) ncl-1(gc53); pept-1(Ig601)* animals were fed ^{35}S labeled OP50 bacteria for 24 hours. Counts per µg proteins extracted from the different strains were plotted. Data represent mean +/− SD (N>=4). * - p<0.0001, 2-tailed unpaired t-test

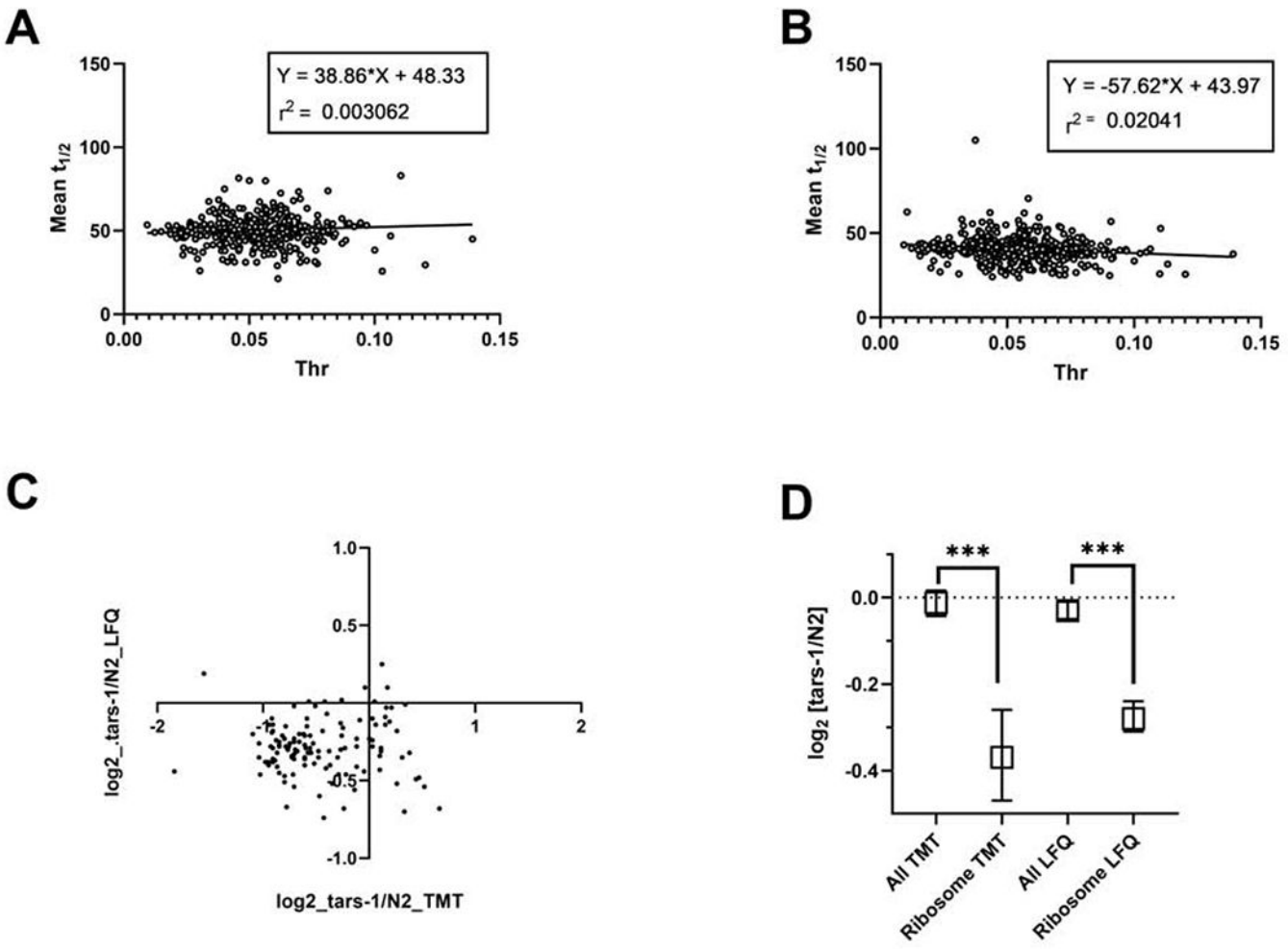

Figure 5. Proteomic analysis of *tars-1*(lf), *larp-1*(lf) *ncl-1*(lf) and *tars-1*(lf); *larp-1*(lf) *ncl-1*(lf) triple mutant combination.

(A,B) SILAC incorporation rate (half-life) plotted against threonine frequency for *tars-1(gc52)* (A) and *tars-1(gc52); larp-1(q783) ncl-1(gc53)* (B). (C) log2[*gc52*/N2] ratio of abundance of ribosomal-related proteins in *tars-1*(*gc52*) versus N2 quantitated by TMT and LFQ methods. (D) log *tars-1*(*gc52*)/N2 ratio of abundance of proteins in entire proteome versus ribosomal-related proteins in by TMT and LFQ methods. See Data S1, Data S2, Figures S5. *** - p<0.001, unpaired 2-tailed t-test

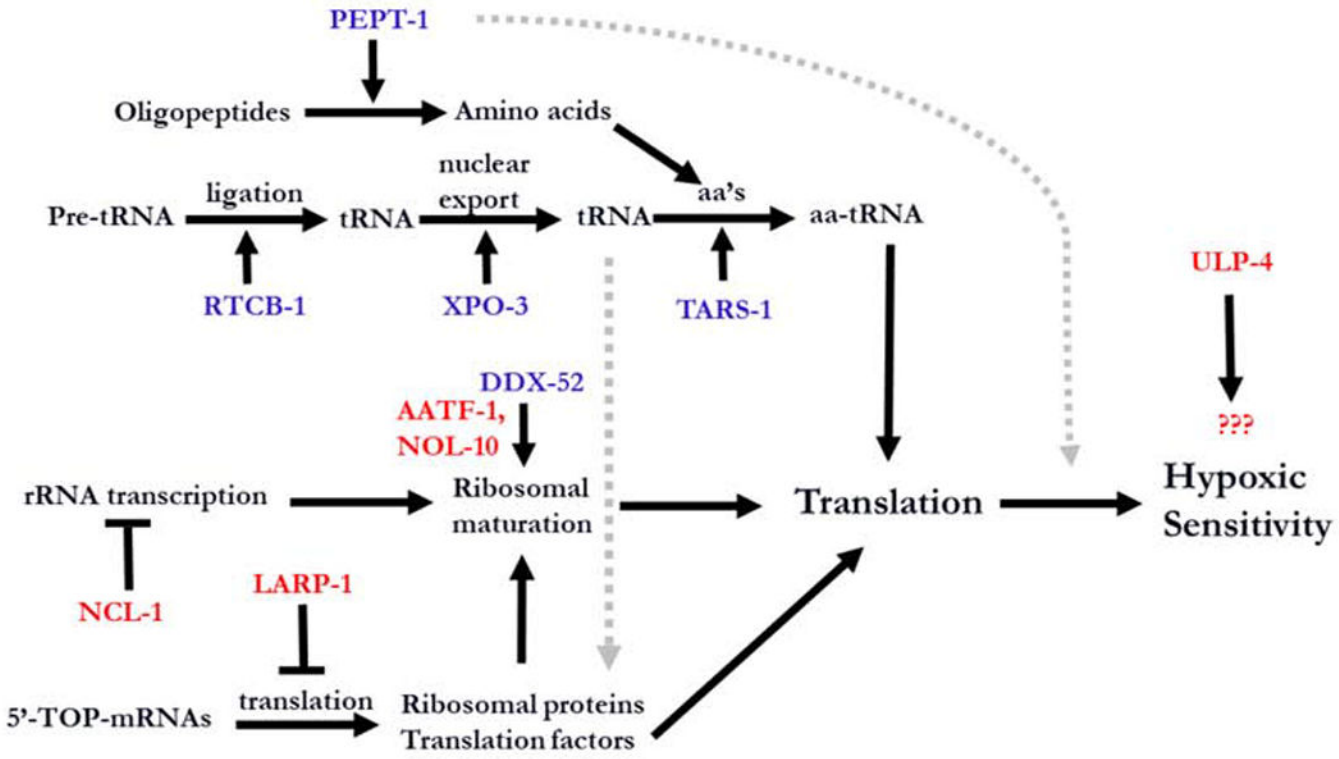

Figure 6. Translational machinery components regulating hypoxia resistance.

Proteins with hypoxia resistant mutants are in purple. Proteins with suppressor mutants are in red. The normal function of the protein is indicated by an arrow (promotes) or by a T-like symbol (inhibition).

Table 1.

Hypoxia-resistant translation mutants

gene	alleles	predicted allele effect	predicted gene function	hypoxic death
pept-1	*gc60*	nonsense, lf	oligopeptide transporter	8.7 ± 4.2
tars-1	*gc52*	splicing, rf	threonyl amino-acyl tRNA synthetase	12.9 ± 2.6
rtcb-1	*gc50*	splicing, rf	tRNA ligase	18.9 ± 5.4
xpo-3	*gc59*	deletion, lf	tRNA export	1.0 ± 1.1
ddx-52	*gc51*	missense, lf	ribosomal RNA helicase	26.3 ± 12.4

Hypoxic death after a 24 hour recovery from a 24 hour hypoxic incubation (n≥3 replicates)

N2 (wild type) hypoxic death =97.2± 2.

See Figure S2

All mutant alleles significantly hypoxia resistant compared to N2 (2-tailed t-test, $p<0.01$)

KEY RESOURCES TABLE

REAGENT or RESOURCE	SOURCE	IDENTIFIER
Antibodies		
Bacterial and Virus Strains		
ET505 bacteria	CGSC	CGSC: 7088
Biological Samples		
Chemicals, Peptides, and Recombinant Proteins		
Lys-C	Promega	Cat#: VA1170
C18 Sep-Pak solid phase extraction cartridges	Waters	Cat#: WAT036945
Endoproteinase LysC	New England Biolabs	Cat#: P8109S
L-Lysine-2HCl, 13C6	ThermoFisher	Cat#: 89988
EZ rich defined medium without lysine	Teknova	Cat#:M2135
Critical Commercial Assays		
BCA Protein Assay Kit	Pierce	Cat#: 23225
TMTsixplex Isobaric Mass Tagging Kit	ThermoFisher	Cat#: 90064
HiFi DNA Assembly Cloning Kit	New England Biolabs	Cat#: E5520S
Deposited Data		
Raw Genomic Sequences	NCBI BioProject	PRJNA555631
Proteomics Data	ProteomeXchange Consortium via Pride Partner Repository	PXD017267
Experimental Models: Cell Lines		
Experimental Models: Organisms/Strains		
C. elegans: N2 (Bristol, wild type)	Caenorhabditis Genetics Center	WBStrain00000001
C. elegans: MC817 *ddx-52(gc51)* I	This Paper	MC817
VC30079 *ddx-52(gk409936)* I	Caenorhabditis Genetics Center	WBStrain00038802
MC805 *tars-1(gc52)* II	This paper	MC805
MC818 *xpo-3(gc59)* IV	This paper	MC818
RB1214 *xpo-3(ok1271)* IV	Caenorhabditis Genetics Center	WBStrain00031915
VC41021 *xpo-3(gk932618)* IV	Caenorhabditis Genetics Center	WBStrain00039984
MC814 *rtcb-1(gc50)* I	This paper	MC814
VC1094 *rtcb-1(gk451) I/hT2 [bli-4(e937) let-?(q782) qIs48]* (I;III)	Caenorhabditis Genetics Center	WBStrain00036319
MC808 *pept-1(gc60)* X	This paper	MC808
BR2742 *pept-1(lg601)* X	Caenorhabditis Genetics Center	WBStrain00003894
MC874 *ncl-1(gc53)* III	This paper	MC874
CF2218 *ncl-1(e1942)* III	Caenorhabditis Genetics Center	WBStrain00004900
JK4545 *larp-1(q783)* III	Caenorhabditis Genetics Center	WBStrain00022648

MC845 *larp-1(gc56)* III	This paper	MC845
MC847 *larp-1(gc57)* III	This paper	MC847
MC894 *ulp-4(gc54)* II	This paper	MC894
MC895 *ulp-4(gc55)* II	This paper	MC895
MC896 *nol-10(gc58)* IV	This paper	MC896
MC907 *aatf-1(gc63gc64)* I	This paper	MC907
CF1038 *daf-16(mu86)* I	Caenorhabditis Genetics Center	WBStrain00004840
CB4856 Hawaiian wild type	Caenorhabditis Genetics Center	WBStrain00004602
MC851 gcIR1 (ddx-52(gc51) I, N2>CB4856)	This paper	MC851
MC836 Ex[pddx-52::ddx-52(+)::GFP pRF4[rol-6(su1006)]	This paper	MC836
MC838 ddx-52(gc51) Ex[pddx-52::ddx-52(+)::GFP pRF4[rol-6(su1006)]	This paper	MC838
Oligonucleotides		
ddx-52 promoter operon amplification forward primer - 5'-gctaacaacttggaaatgaaataCCGGCTGGCCTAGAATATG-3'	This paper	NA
ddx-52 promoter operon amplification reverse primer - 5'-atgccaaggaCATTCCTTTAAAAACGACAAATTGG-3'	This paper	NA
ddx-52 coding amplification forward primer - :5'-taaaggaatgTCCTTGGCATTTAGAACC-3'	This paper	NA
ddx-52 coding amplification reverse primer - 5'-tggccaatcccggggatcctcTATATTCTTATTGTTCTTCTTGATCAAC-3'	This paper	NA
Recombinant DNA		
Software and Algorithms		
Comet – protein ID software	https://sourceforge.net/projects/comet-ms/files/	version 2018.01
PeptideProphet	http://peptideprophet.sourceforge.net/	NA
MassChroQ (version 2.2.12))	[46]	http://pappso.inrae.fr/en/bioinfo/masschroq/
String Clustering software (ver 11.0)	[32]	https://string-db.org/
Other		